8-2000

Spectroscopy and Photometry of Nearby Young Solar Analogs

Eric J. Gaidos
California Institute of Technology

Gregory W. Henry
Tennessee State University

Stephen M. Henry
Tennessee State University

Recommended Citation

E. J. Gaidos et al 2000 AJ 120 1006

SPECTROSCOPY AND PHOTOMETRY OF NEARBY YOUNG SOLAR ANALOGS

E. J. GAIDOS[1,2]

Jet Propulsion Laboratory, California Institute of Technology, 4800 Oak Grove Drive, Pasadena, CA 91109

AND

G. W. HENRY AND S. M. HENRY

Center of Excellence in Information Systems, Tennessee State University, 330 Tenth Avenue North, Nashville, TN 37203-3401

ABSTRACT

We present new photometry and spectroscopy of 34 stars from a catalog of 38 nearby ($d < 25$ pc) G and K dwarfs selected as analogs to the early Sun. We report that the least active star in our sample is also slowly rotating and probably of solar age. Two other stars appear to be evolved objects that have recently acquired angular momentum. A fourth star may be a spectroscopic binary. Many of the other stars belong to previously identified common proper-motion groups. Space motions, lithium abundances, and Ca II emission of these stars suggest ages between 70 and 800 Myr.

Key words: planetary systems — solar system: formation — stars: evolution — Sun

1. INTRODUCTION

Observations of young solar-type stars provide insight into the behavior of the Sun and its effect on the planets during the first few hundred million years of solar system history. Such clues are important in inferring early conditions on the Earth and other planets in the absence of an accessible geologic record. A catalog of 38 nearby stars was constructed for this purpose using published indicators of rapid rotation and high chromospheric activity as proxies of a young age (Gaidos 1998). Here we report results from the analysis of new spectroscopic and photometric data of the 34 stars observable from the northern hemisphere.

2. OBSERVATIONS

Differential photometry of 31 stars was acquired with two automatic photoelectric telescopes (APTs) located at Fairborn Observatory in southern Arizona. A 0.40 m APT (T3) observed 19 of the stars in the Johnson B and V bands, while a 0.75 m APT (T4) observed 12 stars in the Strömgren b and y bands. Details of the 0.40 m APT operation, data reduction procedures, and photometric precision can be found in Henry (1995). A complete discussion of photometry with the 0.75 m APT can be found in Henry (1999).

High-resolution ($R \sim 90,000$) echelle spectra were obtained at the Kitt Peak 0.9 m coudé feed telescope with the F5 camera and 3K × 1K Ford CCD during four observing runs (1998 May, July, and November, and 1999 March). Lower resolution ($R \sim 30,000$) spectra in the region of the Ca II H and K lines were obtained in single-order grating mode. Typical total integration times were ~ 1 hr per star. Spectral images were bias subtracted and flattened with quartz lamp flat fields, and charged particle events were removed by median filtering of multiple exposures. Individual spectral orders were extracted, corrected for sky emission, and wavelength calibrated against thorium-argon arc spectra using the IRAF spectroscopic data reduction package.

3. ANALYSIS

Heliocentric radial velocities were computed through order-by-order comparison of echelle spectra pairs using the Fourier cross-correlation routine FXCOR in IRAF and averaging over many orders. Orders in which the cross-correlation failed because of low stellar signal or the presence of strong telluric emission were excluded. Radial velocities were obtained for 25 solar analogs, including five previously lacking measurements in the literature. Statistical velocity uncertainties estimated using independently calibrated measurements of stars on different nights have a median value of 0.11 km s^{-1}. With our few measurements we cannot distinguish between measurement errors and actual Doppler velocity variations for individual stars. Absolute velocities were calculated by comparison with published higher accuracy values on constant-velocity stars (Duquennoy & Mayor 1991). Multiple velocity measurements of these stars exhibited similar variation, suggesting that the night-to-night differences are measurement errors. The space motions of 36 stars were calculated in right-handed Galactic coordinates with respect to the local standard of rest (LSR), using standard algorithms (Johnson & Soderblom 1987) and solar motion ($+9.00, +11.53, +6.97$) km s^{-1} (Binney & Tremaine 1987; Table 1). The stars have been divided into groups according to their space motions (see § 4). Uncertainties in space motion were calculated using the errors in parallax and proper motion reported in the *Hipparcos* catalog and with an uncertainty in radial velocity, if not known from multiple measurements, taken to be 0.11 km s^{-1}. Our new radial velocity data, combined with previous observations, are sensitive to any variations exceeding 1 km s^{-1} on timescales of ~ 1 yr in 11 stars (Table 1). This is the reflex motion induced by an object of mass m with $m \sin i < 30$ Jovian masses on a 1 AU orbit, where i is the orbital inclination.

The results of our photometric analysis of the APT data[3] are found in Table 2. Many of the stars have observations over more than one observing season, and we analyzed each

---

---

[3] The individual observations are available on the Tennessee State University Automated Astronomy Group Web site at http://schwab.tsuniv.edu/papers/aj/youngsuns/youngsuns.html.

TABLE 1

SPACE MOTIONS

HD	π (mas)	μ_α (mas yr^{-1})	μ_δ (mas yr^{-1})	v_r (km s^{-1})	U (km s^{-1}, LSR)	V (km s^{-1}, LSR)	W (km s^{-1}, LSR)
Ursa Major group:							
26923	47.20	−109.4	−108.3	−7.4	23.2 ± 0.2	11.0 ± 0.1	−2.6 ± 0.3
41593	64.71	−122.3	−103.3	−10.1	19.7 ± 0.1	11.9 ± 0.1	−4.2 ± 0.2
63433[a]	45.84	−9.3	−11.8	−16.1	22.9 ± 0.1	14.0 ± 0.1	−1.0 ± 0.1
72905[a]	70.07	−27.7	87.9	−12.7	18.9 ± 0.1	12.1 ± 0.1	−3.1 ± 0.1
109011.......	42.13	99.7	−13.2	−13.1	23.1 ± 0.8	11.3 ± 0.5	−3.1 ± 0.6
135559[a]	64.19	178.0	−136.5	−3.1	18.7 ± 0.2	12.7 ± 0.1	−6.8 ± 0.2
165185[a]	57.58	105.4	8.0	14.9	23.0 ± 0.1	15.3 ± 0.1	−2.4 ± 0.1
Local association:							
166...........	72.98	379.9	−178.3	−7.0	−5.9 ± 0.2	−10.3 ± 0.2	−2.8 ± 0.2
37394[a]	81.69	2.7	−523.6	2.0	−5.4 ± 1.1	−11.4 ± 0.5	−6.9 ± 0.3
97334[a]	46.04	−248.6	−151.3	−3.7	−6.7 ± 0.3	−11.7 ± 0.5	−4.1 ± 0.2
116956[a]	45.76	−217.4	11.2	−12.3	−7.0 ± 0.3	−6.9 ± 0.2	−1.1 ± 0.1
206860[a]	54.37	231.1	−113.4	−17.0	−5.6 ± 0.2	−10.1 ± 0.1	−3.8 ± 0.3
Possible Pleiades cluster:							
82443[a]	56.35	−147.5	−246.3	8.2	−0.8 ± 0.1	−11.4 ± 0.3	1.6 ± 0.2
113449[b]	45.20	−189.8	−219.6	−11.0	−0.7 ± 0.2	−11.6 ± 0.8	−13.5 ± 0.3
Possible Hyades cluster:							
73350	42.32	−298.4	43.3	35.1	−33.9 ± 0.6	−8.3 ± 0.3	−4.8 ± 0.6
180161[a]	50.00	217.8	408.3	−27.1	−35.0 ± 0.5	−10.6 ± 0.3	−8.4 ± 0.1
High-velocity stars:							
152391[a]	59.04	−711.8	−1483.7	44.9	94.0 ± 0.7	−98.8 ± 1.8	16.4 ± 0.2
220182.......	45.63	636.2	219.2	3.0	−58.6 ± 1.4	−6.4 ± 2.4	4.8 ± 0.7
Old star:							
10780	100.24	582.0	−246.8	2.3	−15.4 ± 0.2	−5.2 ± 0.2	2.0 ± 0.1
Others:							
1237	56.76	433.9	−58.0	...	...	...	...
1835	49.05	394.3	60.5	−2.6	−26.7 ± 0.7	−3.3 ± 0.3	7.1 ± 0.1
7590	42.30	−112.4	−30.5	−13.4	27.4 ± 0.2	7.8 ± 0.1	6.9 ± 0.1
10008	42.35	71.0	−97.7	11.2	4.6 ± 0.1	0.2 ± 0.3	−5.7 ± 0.1
11131	43.47	−122.6	−100.4	−2.1	15.6 ± 0.8	−2.7 ± 1.3	14.4 ± 0.8
20630[a]	109.18	268.9	93.5	18.9	−12.7 ± 0.1	7.1 ± 0.1	2.6 ± 0.1
30495	75.10	130.4	169.2	21.7	−14.9 ± 0.1	2.9 ± 0.1	4.3 ± 0.1
36435	51.10	−148.9	−92.8	12.9	18.4 ± 0.1	8.0 ± 0.1	−11.2 ± 0.1
37394	81.69	2.7	−523.6	2.0	−5.4 ± 1.1	−11.4 ± 0.5	−6.9 ± 0.3
43162[a]	59.90	−47.1	110.9	21.7	−11.3 ± 0.1	1.5 ± 0.1	0.1 ± 0.1
52698	68.42	206.6	40.9	12.2	4.5 ± 0.1	−2.5 ± 0.1	19.0 ± 0.2
59967	45.93	−87.8	53.8	9.0	−2.3 ± 0.1	6.9 ± 0.1	0.2 ± 0.1
72760	45.95	−194.3	23.4	34.5	−26.0 ± 0.3	−7.8 ± 0.1	5.5 ± 0.3
118972.......	64.08	205.9	−166.0	−7.3	17.9 ± 0.2	19.7 ± 0.1	−10.1 ± 0.2
128400[c]	49.15	120.4	−19.4	...	...	...	...
128987[a]	42.43	−111.9	−65.2	−23.0	−13.4 ± 0.2	4.9 ± 0.3	−7.0 ± 0.1
130948[a]	55.73	144.7	32.4	−2.7	13.4 ± 0.1	21.0 ± 0.2	−0.6 ± 0.1
141272[a]	46.84	−176.2	−166.7	−26.6	−10.1 ± 0.1	−16.2 ± 0.5	−6.4 ± 0.1
203244.......	48.86	140.9	169.4	11.5	10.9 ± 0.2	20.5 ± 0.3	−15.5 ± 0.3
217813.......	41.19	−117.7	−28.1	1.5	22.3 ± 0.3	15.5 ± 0.1	9.2 ± 0.1

[a] Constant radial velocity.
[b] Possible spectroscopic binary.
[c] Possible member of Ursa Major group.

season separately. We were able to derive photometric periods for 26 of the 31 stars that we observed with the APTs. These stars all have photometric amplitudes of roughly 0.05 mag or less. The others had amplitudes too small for reliable period determinations. The photometric periods for the individual seasons were determined via standard periodogram techniques that are computatively equivalent to the method of Horne & Baliunas (1986). Periods listed in column (5) are weighted means of the periods determined separately in the B and V bands (for the 0.40 m APT) or in the b and y bands (for the 0.75 m APT). The mean periods listed in column (6) are weighted means of the indi-

vidual periods in column (5). Figure 1 shows the results of the periodogram analysis of HD 63433.

We interpret the photometric periods to be stellar rotation periods. Strong magnetic dynamos in these young, active stars produce sufficient star spot activity for rotational modulation of surface features to be evident in most light curves. Several stars show relatively unchanging rotation periods from year to year (HD 1835, 82443, 113449, and 152391); several others show a range of rotation periods (HD 20630, 30495, 97334, and 206860), which suggests a combination of differential rotation and concentration of star spot activity at different stellar latitudes from year to

TABLE 2
Summary of Photometric Observations and Derived Periods

HD (1)	APT (2)	Date Range (JD − 2,400,000) (3)	N_{obs} (4)	Period (days) (5)	Mean Period (days) (6)
166.........	0.75	49,540–49,740	33	6.23 ± 0.01	6.23
1835	0.75	49,239–49,356	34	7.81 ± 0.01	7.81
		49,546–49,706	29	7.77 ± 0.04	
		49,986–50,092	27	7.68 ± 0.09	
		50,642–50,820	33	7.77[a] ± 0.02	
		51,085–51,197	49	7.88 ± 0.03	
7590	0.40	49,236–49,401	76	5.67 ± 0.01	5.67
10008	0.40	51,172–51,227	34	[b]	...
10780	0.75	49,239–49,389	46	21.0 ± 0.3	21.7
		49,990–50,128	63	22.5 ± 0.4	
11131	0.75	49,239–49,374	56	8.77 ± 0.04	8.92
		49,624–49,724	27	8.90 ± 0.03	
		49,986–50,101	38	9.50 ± 0.06	
20630	0.75	29,239–49,412	66	9.14 ± 0.03	9.20
		49,633–49,773	42	9.14 ± 0.05	
		49,986–50,130	59	9.21 ± 0.04	
		50,391–50,499	31	9.15 ± 0.03	
		50,718–50,868	34	9.10 ± 0.04	
		51,086–51,240	52	9.46 ± 0.03	
26923	0.40	51,172–51,256	48	[b]	...
30495	0.75	49,239–49,408	68	11.47 ± 0.08	11.3
		49,633–49,786	63	11.1 ± 0.1	
		49,986–50,123	53	11.3 ± 0.1	
		50,393–50,510	38	11.45 ± 0.05	
		50,718–50,877	55	11.5 ± 0.2	
		51,087–51,238	57	10.5 ± 0.1	
37394	0.75	49,239–49,449	78	11.02 ± 0.05	10.86
		49,633–49,814	61	10.78 ± 0.05	
		49,986–50,180	74	10.86 ± 0.03	
		50,392–50,551	51	10.84 ± 0.04	
		50,730–50,921	81	[b]	
		51,087–51,283	65	[b]	
41593	0.40	51,170–51,287	73	7.97 ± 0.04	7.97
43162	0.40	51,170–51,261	52	[b]	...
52698	0.40	51,170–51,266	52	[b]	...
63433	0.40	51,170–51,314	109	6.46 ± 0.01	6.46
72760	0.40	51,170–51,317	115	[b]	...
72905[c]	0.75	49,227–49,482	91	4.62 ± 0.01	4.89
				5.28 ± 0.01	
		49,639–49,840	86	4.68 ± 0.01	
				5.30 ± 0.02	
		50,013–50,214	75	4.69 ± 0.01	
		50,405–50,577	60	4.90 ± 0.02	
				5.46 ± 0.02	
		50,736–50,949	83	4.68 ± 0.01	
				5.38 ± 0.01	
		51,096–51,317	73	5.29 ± 0.01	
73350	0.40	51,172–51,316	101	6.14 ± 0.02	6.14
82443	0.40	48,906–49,146	111	5.45 ± 0.01	5.42
		49,272–49,511	165	5.52 ± 0.01	
		49,638–49,878	106	5.40 ± 0.01	
		49,996–50,244	148	5.42 ± 0.01	
		50,392–50,608	145	5.44 ± 0.01	
		50,728–50,976	167	5.39 ± 0.01	
		51,094–51,342	197	5.43 ± 0.01	
97334	0.75	49,095–49,161	41	8.3 ± 0.1	8.25
		49,312–49,519	99	[b]	
		49,687–49,891	72	8.56 ± 0.04	
		50,052–50,252	86	[b]	
		50,404–50,629	57	8.11[a] ± 0.03	
		50,768–50,991	80	8.21 ± 0.05	
		51,123–51,334	53	8.29 ± 0.03	
109011......	0.40	51,170–51,242	67	8.56 ± 0.02	8.81
		51,291–51,360	52	9.19 ± 0.03	

TABLE 2—*Continued*

HD (1)	APT (2)	Date Range (JD − 2,400,000) (3)	N_{obs} (4)	Period (days) (5)	Mean Period (days) (6)
113449.......	0.40	49,321–49,547	124	b	6.54
		49,701–49,908	104	6.53 ± 0.02	
		50,053–50,261	128	6.53 ± 0.01	
		50,419–50,635	105	6.53 ± 0.01	
		50,788–50,993	110	6.56 ± 0.01	
		51,153–51,360	106	b	
116956.......	0.40	51,171–51,360	151	7.80 ± 0.02	7.80
128987.......	0.40	51,181–51,360	114	9.35 ± 0.04	9.35
130948[d]......	0.40	51,172–51,360	139	7.69 ± 0.03	7.85
				7.99 ± 0.03	
135599.......	0.40	51,177–51,360	112	5.97 ± 0.02	5.97
141272.......	0.40	51,183–51,360	114	14.01 ± 0.04	14.01
152391.......	0.75	49,095–49,163	31	11.5 ± 0.1	11.5
		49,399–49,547	36	b	
		49,755–49,904	29	11.4 ± 0.1	
		50,161–50,257	31	11.5 ± 0.1	
		50,490–50,642	41	11.4 ± 0.1	
		50,857–50,995	45	11.5 ± 0.1	
		51,223–51,341	40	b	
180161.......	0.40	51,233–51,359	74	9.7 ± 0.1	9.7
206860.......	0.75	49,126–49,337	65	4.73 ± 0.01	4.91
		49,491–49,706	54	4.64 ± 0.01	
		49,862–50,071	43	5.10 ± 0.01	
		50,392–50,443	20	e	
		50,620–50,806	37	5.18 ± 0.01	
		51,077–51,179	48	4.68 ± 0.04	
217813.......	0.75	49,145–49,362	51	b	8.05
		49,512–49,666	30	8.04 ± 0.01	
		49,879–50,091	57	8.10 ± 0.02	
220182.......	0.40	51,172–51,360	48	7.66 ± 0.01	7.66

[a] Period and its error have been multiplied by two.
[b] Photometric variability too small to determine period.
[c] Both the 4.7 and 5.3 day–periods often appear in the same observing season.
[d] Both periods appear in the same observing season.
[e] Insufficient data to determine period.

year. Two stars (HD 72905 and HD 130948) show two prominent rotation periods in the *same* observing season.

New and previously reported spectroscopic measurements appear in Table 3. Luminosities, L, are from *Hipparcos* parallax and visual magnitude measurements (Perryman et al. 1997) and an empirical bolometric correction (Flower 1996). Effective temperatures, T_{eff}, were estimated from the relation of Flower (1996). The emission in the Ca II H and K lines, a well-established indicator of stellar chromospheric activity, is expressed in terms of the Mount Wilson index,

$$S_{MW} = 12a \frac{C_K + C_{KH}}{C_V + C_R}, \qquad (1)$$

where C_K and C_{KH} are the total measured signal in two triangular passbands, each with FWHM of 1.09 Å and centered on the K and H line cores, and C_V and C_R are the measured signal in 20 Å–wide regions of the continuum blueward and redward of the lines (Vaughan, Preston, & Wilson 1978). The constant $a \approx 0.76$, which incorporates spectral response differences between the KPNO coudé echelle and the original Mount Wilson spectrophotometer, was obtained by comparing our measurements with known S values for three sample stars (HD 1835, 30495, and 72905) listed in Table 3 of Duncan et al. (1991). The index R'_{HK}, the

logarithmic flux ratio of Ca II in emission to the bolometric flux of the photosphere, was calculated from the S_{MW} values of each star (Noyes et al. 1984). Calibration errors are created by the long-term variability in the S index, 0.02–0.03 for the calibration stars (Radick et al. 1998; Wilson 1978). We estimate our R'_{HK} values have an absolute uncertainty of 0.03–0.05 due to calibration errors alone. Thus while our measurements are not appropriate for sensitive estimates of variability, they are sufficient to distinguish clearly active from relatively inactive (Sun-like) stars. Values of this index and revised values of the logarithmic index of coronal X-ray flux relative to bolometric flux R_X from Gaidos (1998) are reported in Table 3.

Spectroscopy in the vicinity of the 6707.8 Å line of Li I was obtained for 34 stars and is reported in Table 3. The equivalent widths of the blended Li I lines in the vicinity of 6707.8 Å were obtained by least-squares fitting of a model that included the Li I doublet at 6707.761 and 6707.912 Å, two Fe I doublets at 6703.568 and 6705.101 Å, and two Fe I lines at 6707.441 and 6710.316 Å. The strength of each of the iron lines was independently fitted except for the line at 6707.441 Å, which is often blended with the Li I lines in the spectra of these rapidly rotating stars. Thus we fixed the intensity of this line relative to one of the Fe I lines, estimating the scaling factor from spectra of lithium-depleted old stars. This scaling factor is not constant but varies with the
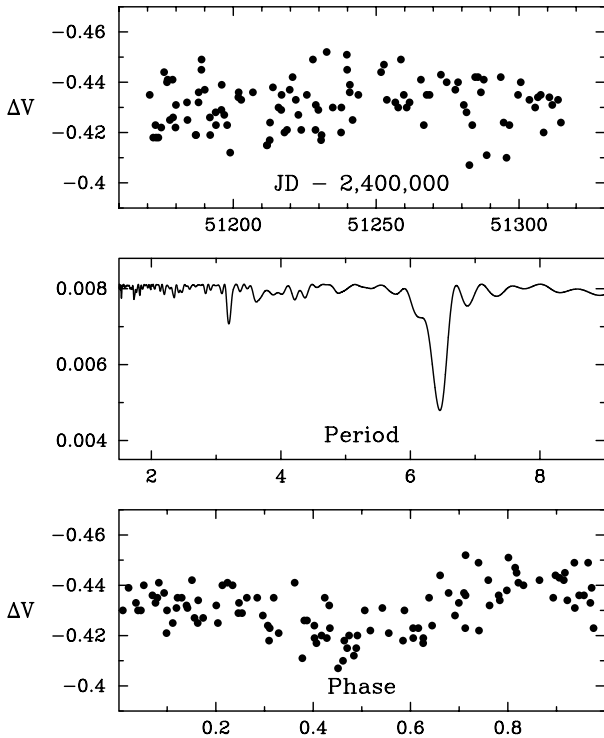
FIG. 1.—*Top*: Johnson *V* photometric observations of HD 63443 plotted against the Julian Date. *Middle*: Periodogram of the HD 63443 observations. The sum of the squares of the residuals from a least-squares sine fit are plotted against the trial period in days. The resulting period is 6.46 ± 0.01 days. *Bottom*: The photometric observations from the top panel plotted against the photometric phase computed with the 6.46 day period and the arbitrary epoch JD 2,451,170.

stellar $T_{\rm eff}$. However, this effect is important only when Li I lines are very weak. A correction of 3.5% was applied to the equivalent widths to account for scattered light (J. Cardelli 1994, unpublished). Errors in the equivalent width of the lithium line are typically ~ 1 mÅ. For consistency, abundance estimates with respect to hydrogen were estimated from interpolations of the curve of growth published by Soderblom et al. (1993). Lithium abundances relative to hydrogen ($\log N = 12$) and values obtained by Pasquini, Liu, & Pallavicini (1994) for two southern stars not observed by us are given as well.

The projected rotational velocity ($v \sin i$) of each star A was estimated by cross-correlating its spectrum with that of a more slowly rotating template star B. The additional broadening due to the more rapid rotation of A is the difference in quadrature between the width of the correlation peak $\sigma_{\rm AB}$ and the width of the autocorrelation peak $\sigma_{\rm BB}$. Differencing the widths of the correlation and autocorrelation spectra removes the contribution of intrinsic line widths and instrument broadening. The $v \sin i$ value is calculated by adding the rotational velocity of the template in quadrature to the result,

$$(v \sin i)_{\rm A} = \sqrt{\sigma_{\rm AB}^2 - \sigma_{\rm BB}^2 + (v \sin i)_{\rm B}^2} \ . \qquad (2)$$

Estimates for stars with multiple measurements are averaged. The mean measurement error in $v \sin i$ is 0.28 km but the rms differences between multiple measurements averaged over all stars is 0.63 km s^{-1}. The observed inclination of the star with respect to the line-of-sight (0 indicates pole-on) was computed from our measured $v \sin i$ values and

rotation periods, along with each star's radius estimated from its luminosity and $T_{\rm eff}$. The range of possible inclinations for each star listed in Table 3 reflects the uncertainties in all of these parameters. Most of the uncertainty comes from the $v \sin i$ measurements. We included an additional error of 0.5 km s^{-1} in $v \sin i$ to account for uncertainties in the microturbulence parameter.

4. DISCUSSION

Radial velocity measurements now rule out close ($a < 1$ AU) stellar-mass companions with $\sin i > 20°$ around 16 stars (Table 1). One star (HD 113449) may be a spectroscopic binary, exhibiting a change of 20 km s^{-1} in 10 months. Measurements using low-resolution (3.6 km s^{-1} accuracy) prism spectra obtained at two epochs also suggest velocity variation (Moore & Paddock 1950), but additional confirming observations are needed. If this star is a spectroscopic binary, by the criteria of Gaidos (1998) this system should *not* be considered a solar analog. We confirm the constant and anomalously high motions of HD 152391 and HD 220182 (137 and 59 km s^{-1}, respectively). The radial velocity of a third star (HD 73350) was erroneously reported (Gaidos 1998), and although its correct space motion is high (35 km s^{-1}), it is not anomalous.

The remaining 34 stars with known space motions are plotted in Figure 2. Integrals of the motion reflect the ancestral dynamics of a star and any subsequent perturbations by close encounters with other stars and molecular clouds. Within the restricted (25 pc radius) volume of the sample space, velocities are quantitative proxies for the three integrals of motion describing nearly circular orbits in the axisymmetric gravitational potential of the Galactic disk, i.e., $E_z = 1/2(V^2 + \kappa_0^2 y^2)$, $E_z = 1/2(W^2 + v_0^2 z^2)$, and $L = U + y\Omega_0$, where y and z are the right-handed Galactic coordinate distances from the Sun, κ_0 and v_0 are the epicycle frequencies evaluated at the LSR, and Ω_0 is the angular velocity of the LSR (Binney & Tremaine 1987). Since the coefficients κ_0, v_0, and Ω_0 are small, with estimated values of 0.036, 0.100, and 0.014 km s^{-1} pc^{-1}, respectively, the spatial terms in the integrals of motion can be neglected compared to the velocity terms. In the following discussion, we consider these stars according to the their clustering into common-motion groups.

The short rotation periods and high Ca II HK emission of these objects relative to the Sun (Fig. 3) are consistent with their selection as active stars with exceptionally X-ray luminous coronae, with one exception (discussed below). The X-ray emission of these stars exhibits considerable scatter from the empirical relation with rotation $L_{\rm X} \sim P^{-2.46}$ formulated by Güdel, Guinan, & Skinner (1997; *solid line*). X-ray and Ca II emission are also not strongly correlated. This may in part be due to variability in activity and the 8–9 yr that elapsed between the X-ray measurements and the Ca II HK measurements. The photospheric lithium abundances are plotted in Figure 4, where the stars are identified according to their space motion group affiliation, if any. The Li abundance of stars in the Pleiades (65 Myr; Soderblom & Mayor 1993) and Hyades (650 Myr; Perryman et al. 1998) dwarfs are shown for comparison. The values are typical of stars with ages within this range and follow the well-established inverse trend with $T_{\rm eff}$.

Seven young solar analogs (Table 3) move within 5 km s^{-1} of a mean motion consistent with the previously described Ursa Major kinematic group (Soderblom &

TABLE 3

ACTIVITY, LITHIUM, AND ROTATION

HD	L ($L_\odot$)	$T_{\rm eff}$ (K)	$R_{\rm X}$	$R'_{\rm HK}$	W_{6708} (mÅ)	log N(Li) (H = 12)	$v \sin i$ (km s^{-1})	i (deg)
Ursa Major group:								
26923	1.10	6010	−4.64	−4.52	79.2 ± 3.4	2.73 ± 0.09	4.2	...
41593	0.45	5360	−4.59	−4.36	12.8 ± 3.5	1.22 ± 0.17	5.0	50−90
63433	0.73	5580	−4.55	−4.34	78.9 ± 2.3	2.33 ± 0.10	6.1	40−90
72905	0.97	5820	−4.47	−4.42	108.5 ± 5.0	2.80 ± 0.10	8.7	45−90
109011	0.35	4760	−4.74	−4.36	24.7 ± 3.4	0.81 ± 0.15	5.5	55−90
135599	0.40	5080	−4.94	...	3.7 ± 1.9	0.34 ± 0.28	4.6	30−65
165185	1.08	5810	−4.51	−4.49	92.7 ± 3.3	2.65 ± 0.10	7.2	...
Local association:								
166	0.65	5310	−4.38	−4.38	71.2 ± 0.5	1.98 ± 0.11	4.1	20−45
37394	0.48	5200	−4.74	−4.44	1.3 ± 3.2	0.03 ± 0.03	4.0	45−90
97334	1.08	5890	−4.57	−4.41	81.1 ± 2.8	2.64 ± 0.09	5.6	45−90
116956	0.55	5170	−4.48	...	31.0 ± 2.6	1.42 ± 0.12	5.6	45−90
206860	1.17	5930	−4.46	−4.41	100.8 ± 3.7	2.81 ± 0.09	9.4	45−90
Possible Pleiades cluster:								
82443	0.45	5240	−4.01	−4.22	183.9 ± 2.8	2.61 ± 0.12	6.1	35−90
113449	0.41	5020	−4.41	...	139.8 ± 2.7	2.08 ± 0.12	5.8	40−90
Possible Hyades cluster:								
73350	0.97	5750	−4.85	−4.49	36.0 ± 3.5	2.09 ± 0.10	3.8	20−40
180161	0.58	5170	−4.67	−4.44	9.3 ± 1.6	0.86 ± 0.14	3.1	25−60
High-velocity stars:								
152391	0.58	5230	−4.63	−4.44	6.4 ± 2.4	0.77 ± 0.21	3.7	40−90
220182	0.52	5150	−4.59	−4.34	47.3 ± 3.6	1.59 ± 0.12	5.0	40−90
Old star:								
10780	0.53	5420	−4.89	−4.71	1.3 ± 2.21	0.27 ± 0.27	2.0	35−90
Others:								
1237	0.66	5340	−4.46	−4.44	...	...	0.0	...
1835	1.00	5860	−4.55	−4.46	76.7 ± 4.1	2.58 ± 0.10	...	...
7590	1.08	5930	−4.72	−4.46	92.1 ± 4.3	2.75 ± 0.10	6.4	35−65
10008	0.46	5170	−4.48	−4.38	88.7 ± 2.3	1.96 ± 0.12	2.9	...
11131	0.92	5790	−4.37	−4.47	64.5 ± 3.3	2.42 ± 0.10	...	...
20630	0.85	5660	−4.65	−4.44	35.0 ± 3.6	2.00 ± 0.11	4.5	40−90
30495	0.97	5830	−4.77	−4.56	47.0 ± 3.5	2.29 ± 0.10	4.1	45−90
36435	0.56	5460	−4.74	−4.44	23.0 ± 5.0	1.60 ± 0.15	...	...
43162	0.71	5480	−4.31	−4.40	60.3 ± 2.7	2.07 ± 0.11	5.7	...
52698	0.45	4930	−4.75	−4.59	0.2 ± 3.0	...	3.5	...
59967	0.88	5730	−4.48	−4.44	81.4 ± 3.6	2.50 ± 0.10	3.4	...
72760	0.53	5210	−4.78	−4.39	4.4 ± 3.3	0.57 ± 0.45	4.2	...
118972	0.42	4990	−4.67	−4.40	3.7 ± 3.4	0.24 ± 0.29	5.2	...
128400	0.75	5480	−4.83	−4.56	...	...	...	...
128987	0.63	5590	−4.78	...	25.8 ± 2.3	1.78 ± 0.11	3.2	30−80
130948	1.21	5730	−4.69	−4.45	98.4 ± 2.4	2.61 ± 0.10	6.0	40−90
141272	0.46	5170	−4.62	...	3.9 ± 1.9	0.48 ± 0.27	4.0	70−90
203244	0.61	5530	−4.61	−4.39	22.0 ± 5.0	1.64 ± 0.15	...	...
217813	1.09	5810	−4.55	−4.47	78.0 ± 3.4	2.54 ± 0.10	3.1	20−40

Mayor 1993) at $(U, V, W) = (+2.4, +12.2, -3.3)$ km s^{-1} (Fig. 2). The age of the Ursa Major comoving group has been estimated as 300 Myr, based on several techniques (Giannuzzi 1979). The lithium abundances of the seven members are intermediate between those of the Pleiades (70 Myr) and Hyades (625 Myr) dwarfs, and thus consistent with the estimated age. Five stars have motions within 3 km s^{-1} of a mean of $(-6.1, -10.1, -3.7)$ km s^{-1}, consistent with previous descriptions of a local association (Jeffries 1995). A link between the Local Association and the Pleiades Cluster has been proposed (Eggen 1998 and references therein). We estimate a mean space motion of the Pleiades cluster of $(+8.6, -1.0, +1.4)$ based on a mean radial velocity of 5.85 km s^{-1} and *Hipparcos* proper motions of 17 of its brightest members (Eggen 1998). This motion is significantly different ($\Delta U = 8.8$ km s^{-1}) from

that of the Local Association, and we continue to believe that these two groups are kinematically distinct entities. Furthermore, none of the five Local Association stars in this sample have the characteristics expected of Pleiades-age, solar-mass stars, i.e., log $L_{\rm X} \sim (-3.5)$ and log N(Li) ~ 3. Rather, our data suggest that the Local Association is a group of stars similar in age to the Ursa Major group. However, the TW Hydra association, a group of low-mass stars that includes the 10 to 20 Myr–old T Tauri archetype (Kastner et al. 1997; Webb et al. 1999; Sterzik et al. 1999) appears to move at $(-4.3, -9.4, -2.5)$ km s^{-1}, i.e., within about 2 km s^{-1} of the Local Association. More accurate proper-motion measurements of TW Hya stars are needed. A common motion would indicate either a common origin of the two groups (although not a common age) or suggest that young stars in the solar neighborhood tend to form
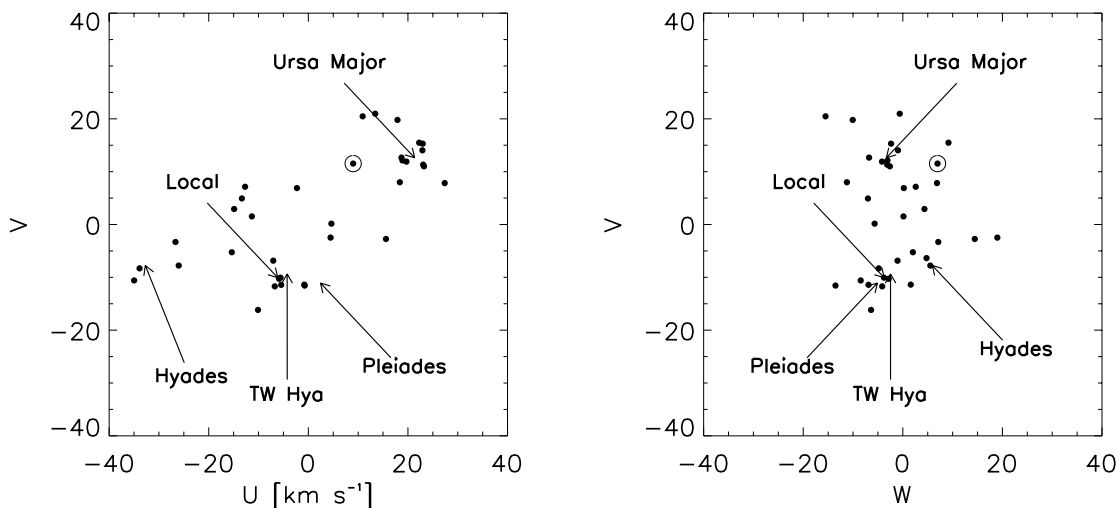
Fig. 2.—Space motions of 34 of the 38 young solar analogs with respect to the LSR. Two stars in the sample (HD 1237 and HD 128400) lack radial velocity information, and two others (HD 152391 and HD 220182) have anomalously high space motions that fall outside the plot. The Sun is shown as the encircled point. The motions of the Ursa Major, Local Association, and TW Hydra kinematic groups and the Pleiades and Hyades clusters are labeled.

with the same motion, perhaps that of a local molecular cloud component of the disk (the Ursa Major Group being a clear exception).

HD 82443 (DX Leo) is an exceptionally active star in our survey that moves within 7.4 km s^{-1} of the Pleiades and 5.7 km s^{-1} of the TW Hydra association. The common motion of HD 82443 and the Pleiades was pointed out by Soderblom & Clements (1988), and the observed lithium abundance, rapid rotation, high Ca II HK emission, and high X-ray luminosity (by far the highest in the sample) support an exceptionally young age. Its apparent rotation period was observed to vary from 5.39 to 5.52 days, consistent with

a previous estimate (Messina et al. 1999). We derive a value of $v \sin i$ of 6.1 ± 0.2 km s^{-1}, in agreement with Benz & Mayor (1981). The (U, V)-space motions of HD 113449 also lie within the range 3–4 km s^{-1} of the Pleiades and the Local Association. This could be merely a coincidence if the system is a single-lined spectroscopic binary; however, the high lithium abundance suggests a Pleiades age as well. Stars in the Hyades cluster, 46 pc distant, have been identified as far as 20 pc from the cluster center (Perryman et al. 1998), and thus members of this ~625 Myr–old cluster may appear in our sample. Two stars, HD 73350 and HD 180161, have (U, V)-space motions within 4 km s^{-1} of the mean cluster motion of $(-32.7, -7.8, +5.9)$ with respect to the LSR, although the W-components of their motion differ by 10–15 km s^{-1}. Their rotation, activity and lithium abundances suggest a Hyades-like age.
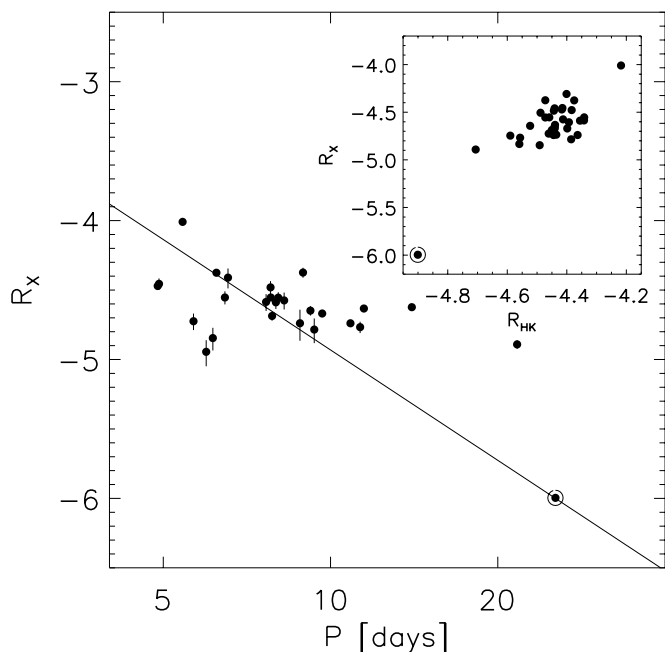

Fig. 3.—Index of coronal X-ray emission R_X plotted vs. rotation period for young solar analogs. The solid line represents the empirical relation from Güdel, Guinan, & Skinner (1997). The inset shows the correlation between X-ray emission and the equivalent index for emission in the Ca II K and H lines. The encircled point is the Sun.
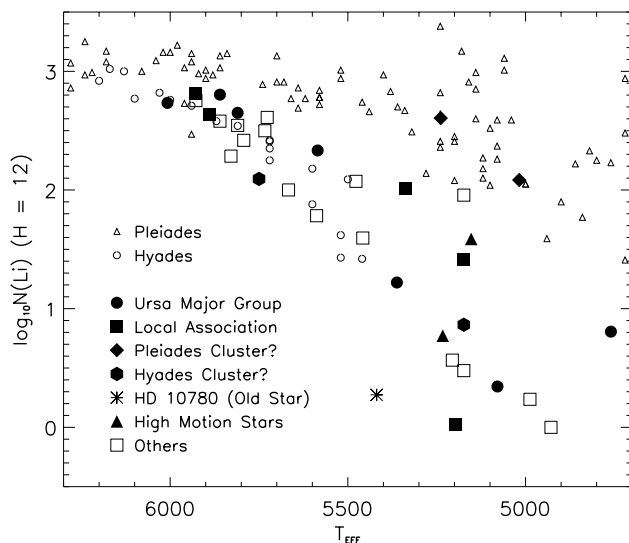

Fig. 4.—Lithium abundances relative to hydrogen for 34 solar analogs estimated from the strength of the Li I doublet at 6707.8 Å. Dwarf stars in the 70 Myr–old Pleiades (Soderblom et al. 1993) and 625 Myr–old Hyades (Soderblom et al. 1990) clusters are shown for comparison.

The K0 star HD 10780 has a rotation period of 21.67 days, much longer than the other stars in the sample, indicative of a solar age. For example, Lachaume et al. (1999) assigned an age of 2.2–3.5 Gyr, based on a previous measurement of 23 days (Noyes et al. 1984). A long rotation period, combined with a nearly pole-on–viewing geometry, would explain the very low $v \sin i$ value 0.6 km s^{-1} (Fekel 1997). From an estimate of the FWHM of 0.10 Å from our new spectra, the *total* broadening in the stellar spectrum is 2 km s^{-1}. This is roughly equal to an estimate of the macroturbulence parameter (Saar & Osten 1997). Thus the actual value of $v \sin i$ for HD 10780 could be even smaller. The star is not a member of any of the identified kinematic groups. Its lithium abundance is roughly solar, also suggesting an old age. However, the observed Ca II emission index $S = 0.26$ (cf. the value of 0.32 found by Duncan et al. in 1979) exceeds the solar maximum value by 10 times the normal solar variation (Radick et al. 1998). Likewise, HD 10780 is 10 times more X-ray luminous than the Sun at solar maximum ($R_X \approx -5.8$). As the optical and X-ray data were obtained at different epochs, the different observations cannot be explained by a single flare event. Radial velocity data rule out stellar companions on nearly circular orbits closer than 10 AU. A spectrum of SAO 11985, a putative $m_V = 9.69$ companion 48" from HD 10780, reveals that it is a more distant giant star with line-of-sight velocity 36 km s^{-1} relative to HD 10780 and is unlikely to be the source of X-ray emission. Regardless, a companion could not explain the Ca II HK emission. Since there is no evidence that the Sun's activity is anomalous with respect to other solar-mass stars of its age (Soderblom 1983), we conclude that HD 10780 is a relatively active star of solar age and not a young analog. In fact, the reestimated value of R_X falls just below the original selection cutoff of Gaidos (1998).

An explanation for the nature of the two high-velocity stars (HD 152391 and HD 220182) in our sample remains elusive. Their space motions and their location well above the zero-age main sequence suggest that these are evolved stars from an old disk or halo population. Radial velocity measurements at multiple epochs (ours and those in the literature) rule out the possibility that either of these objects are spectroscopic binaries. Moreover, the high Ca II HK emission, short rotation periods, and high $v \sin i$ values unambiguously confirm that each star (and not some unknown companion) is active. Even more enigmatic is the high abundance of lithium in HD 220182 (log N(Li) ≈ 1.6), characteristic of an age of 200–300 Myr rather than ~10 Gyr. It would appear that the convecting outer layers of these stars have recently acquired a source of angular momentum, and in one case, lithium. Simon & Drake (1989) proposed that the rapid rotation and high chromospheric activity seen in a small fraction of G and K giant and subgiant stars is the result of convective dredge-up of material from a rapidly rotating core as the stars evolve to the base of the red giant branch. The high lithium abundance seen in asymptotic giant branch stars has been explained by lithium production via decay of ^{7}Be (Cameron & Fowler 1971) and rapid convective transport to the surface (Fekel & Balachandran 1993), but this mechanism may not be responsible for all cases (King, Deliyannis, & Boesgaard 1996). It is not clear whether the required temperatures are reached in evolved, low-mass stars. Alternatively, Siess & Livio (1999) have proposed that the high rotation rates, chromospheric activity, and lithium abundance seen in a small fraction of G and K giant stars can be explained by consumption of substellar companions. The accretion of a 1–2 Jovian mass planet from a decaying orbit onto an old main-sequence star might explain the anomalous observations described here.

REFERENCES

Benz, W., & Mayor, M. 1981, A&A, 93, 235
Binney, J., & Tremaine, S. 1987, Galactic Dynamics (Princeton: Princeton Univ. Press)
Cameron, A. G. W., & Fowler, W. A. 1971, ApJ, 164, 111
Duncan, D. K., et al. 1991, ApJS, 76, 383
Duquennoy, A., & Mayor, M. 1991, A&A, 248, 485
Eggen, O. J. 1998, AJ, 116, 1810
Fekel, F. C. 1997, PASP, 109, 514
Fekel, F. C., & Balachandran, S. 1993, ApJ, 403, 708
Flower, P. J. 1996, ApJ, 469, 355
Gaidos, E. J. 1998, PASP, 110, 1259
Giannuzzi, M. A. 1979, A&A, 77, 214
Güdel, M., Guinan, E. F., & Skinner, S. L. 1997, ApJ, 483, 947
Henry, G. W. 1995, in ASP Conf. Ser. 79, Robotic Telescopes: Current Capabilities, Present Developments, and Future Prospects for Automated Astronomy, ed. G. W. Henry & J. A. Eaton (San Francisco: ASP), 44
———. 1999, PASP, 111, 845
Horne, J. H., & Baliunas, S. L. 1986, ApJ, 302, 757
Jeffries, R. D. 1995, MNRAS, 273, 559
Johnson, D. R. H., & Soderblom, D. R. 1987, AJ, 93, 864
Kastner, J. H., Zuckerman, B., Weintraub, D. A., & Forveille, T. 1997, Science, 277, 67
King, J. R., Deliyannis, C. P., & Boesgaard, A. M. 1996, AJ, 112, 2839
Lachaume, R., Dominik, C., Lanz, T., & Habing, H. J. 1999, A&A, 348, 897
Messina, S., Guinan, E. F., Lanza, A. F., & Ambruster, C. 1999, A&A, 347, 249

Moore, J. H., & Paddock, G. F. 1950, ApJ, 112, 48
Noyes, R. W., Hartmann, L. W., Baliunas, S. L., Duncan, D. K., & Vaughan, A. H. 1984, ApJ, 279, 763
Pasquini, L., Liu, Q., & Pallavicini, R. 1994, A&A, 287, 191
Perryman, M. A. C., et al. 1998, A&A, 331, 81
———. 1997, A&A, 323, L49
Radick, R. R., Lockwood, G. W., Skiff, B. A., & Baliunas, S. L. 1998, ApJS, 118, 239
Saar, S. H., & Osten, R. A. 1997, MNRAS, 284, 803
Siess, L., & Livio, M. 1999, MNRAS, 308, 1133
Simon, T., & Drake, S. A. 1989, ApJ, 346, 303
Soderblom, D. R. 1983, ApJS, 53, 1
Soderblom, D. R., & Clements, S. D. 1988, AJ, 95, 580
Soderblom, D. R., Jones, B. F., Balachandran, S., Stauffer, J. R., Duncan, D. K., Fedele, S. B., & Hudon, J. D. 1993, AJ, 106, 1059
Soderblom, D. R., & Mayor, M. 1993, AJ, 105, 226
Soderblom, D. R., Oey, M. S., Johnson, D. R. H., & Stone, R. P. S. 1990, AJ, 99, 595
Sterzik, M. F., Alcalá, J. M., Covino, E., & Petr, M. G. 1999, A&A, 346, L41
Vaughan, A. H., Preston, G. W., & Wilson, O. C. 1978, PASP, 90, 267
Webb, R. A., Zuckerman, B., Platais, I., Patience, J., White, R. J., Schwartz, M. J., & McCarthy, C. 1999, ApJ, 512, L63
Wilson, O. C. 1978, ApJ, 226, 379